HAdV protein V core protein is targeted by the host SUMOylation machinery to limit essential viral functions

Nora Freudenberger[1,2], Tina Meyer[2], Peter Groitl[1], Thomas Dobner[2] and Sabrina Schreiner*[1]

[1] Institute of Virology, Technische Universität München/Helmholtz Zentrum München, Munich, Germany

[2] Heinrich Pette Institute, Leibniz Institute for Experimental Virology, Hamburg, Germany

* Corresponding author: Phone: +49 89 3187 3466
Fax: +49 89 3187 3329
Email: sabrina.schreiner@tum.de

Running title: protein V SUMO conjugation deregulates HAdV gene expression

Keywords: human adenovirus, HAdV, protein V, core, SUMO, PML-NB

Abstract

Human Adenoviruses (HAdV) are non-enveloped containing a linear, double-stranded DNA genome surrounded by an icosahedral capsid. To allow proper viral replication, the genome is imported through the nuclear-pore-complex associated with viral core proteins. Until now, the role of these incoming virion proteins during the early phase of infection was poorly understood.

The core protein V is speculated to bridge core and the surrounding capsid. It binds the genome in a sequence-independent manner and localizes in the nucleus of infected cells, accumulating at nucleoli. Here, we show that protein V contains conserved SUMO conjugation motifs (SCMs). Mutation of these consensus motifs resulted in reduced SUMOylation of the protein; thus protein V represents a novel target of the host SUMOylation machinery. To understand the role of protein V SUMO posttranslational modification during productive HAdV infection, we generated a replication-competent HAdV with SCM mutations within the protein V coding sequence. Phenotypic analyses revealed that these SCM mutations are beneficial for adenoviral replication. Blocking protein V SUMOylation at specific sites shifts the onset of viral DNA replication to earlier time points during infection and promotes viral gene expression. Simultanously, these altered kinetics within the viral life cycle are accompanied by more efficient proteasomal degradation of host determinants and increased virus progeny production than observed during wildtype infection.

Taken together, our studies show that protein V SUMOylation reduces virus growth; hence, protein V SUMOylation represents an important novel aspect of the host

antiviral strategy to limit virus replication and thereby points to potential intervention strategies.

Importance

Many decades of research have revealed that HAdV structural proteins promote viral entry and mainly physical stability of the viral genome in the capsid. Our work over the last years showed that this concept needs expansion, as the functions are more diverse. We showed that capsid protein protein VI is regulating antiviral response by modulation of the transcription factor Daxx during infection. Moreover, core protein VII interacts with SPOC1 restriction factor, being beneficial for efficient viral gene expression. Here, we were able to show that also core protein V represents a novel substrate of the host SUMOylation machinery and contains several conserved SCMs; mutation of these consensus motifs reduced SUMOylation of the protein. Unexpectedly, we observed that introducing these mutations into HAdV promotes adenoviral replication. Conclusively, we offer novel insights into adenovirus core proteins and provide evidence that SUMOylation of HAdV factors regulates replication efficiency.

Introduction

Human adenoviruses (HAdV) show considerable tissue tropism, but the primary targets are terminally differentiated epithelial cells. This results in a broad spectrum of clinical symptoms with HAdV as the causative agent (1). Usually, an HAdV infection is mild and self-limiting. However, in rare cases the course of infection can be severe. Worst affected by such complications are newborns or immuno-compromised patients, e.g. those suffering from AIDS or having received an organ transplant (2). The latter presents a serious problem, since no specific treatment is yet available against adenoviral infections. Hence, the therapy during severe infection courses can only be symptomatic and not uncommonly results in the death of a patient, as there is no specific treatment available against adenoviral infections.

Little structural information exists about the adenoviral core. It contains three highly basic proteins, which bind the viral genome in a sequence unspecific manner, the major core protein VII (VII), the minor core protein V (V) and the small peptide μ (μ, X) (3). All of them are encoded by distinct mRNAs of the L2 family (4).

Within all adenovirus genera, minor core protein V is specific for *Mastadenoviruses*. It has a length of 368 amino acids with a calculated molecular weight of 41 kDa (5). Protein V is present in ~157 copies per virion and speculated to bridge the viral core with the surrounding capsid through its interaction with capsid protein VI (5). Moreover, early cross-linking studies indicated that protein V exists in a complex with VII, μ or both proteins together; VII and μ could not be detected in complexes without V (5). It was further shown that protein V is able to dimerize in solution (6). Based on these findings, a model was proposed for the stoichiometric adenosome (nucleosome-like state of the viral genome) organization where the viral DNA wraps

around six molecules of protein VII, which are interspaced by one molecule of protein V. However, the position of protein μ in this condensed DNA structure remains elusive (3). Complexes between protein V and DNA have been shown to be very stable. Due to its ability to facilitate interactions between the other core proteins and the viral genome, protein V is speculated to have functions similar to those of cellular histone 1 (H1) (6).

So far, no functional domains could be identified within the primary sequence of protein V. However, it contains several regions that target the protein to the nucleus (NLS) as well as to the nucleolus (NoLS) of infected host cells. The N-terminal motif (aa 23-78) and the C-terminal motif (aa 315-337) target the protein to the nucleoli as well as to the nucleoplasm independently of each other. In contrast, the central NLS can only mediate localization of protein V in the nucleoplasm (7). Indeed, newly synthesized protein V is found exclusively in the nucleus during HAdV infection where it also colocalizes with nucleoli, but spares adenoviral replication centers (7). Protein V was found to induce the relocalization of two major nucleolar proteins, nucleolin (C23) and nucleophosmin (B23/NPM1), to the cytoplasm during transfection experiments (7).

Several studies investigated the behavior of incoming protein V within the first hours of HAdV infection. Predominantly performed with high moi, they agree on a rapid transport of protein V to the host nucleus, where it immediately partially associates with nucleoli (8) . However, Puntener and coworkers claim that protein V does not enter the nucleus early after infection. They propose that it dissociates in two sequential steps. The first fraction of protein V is released from the viral particle when it is released from an endosome to the cytoplasm. This process is assumed to

be associated with the disassembly of the capsid vertices. The second fraction of protein V is released during final capsid uncoating at the NPC and could not be observed inside the nucleus afterwards. Consequently, the viral genome translocation is proposed to follow in a complex with core protein VII, but not with protein V (9). Regarding the latter step, Hindley and coworkers come to a similar conclusion. However, they can detect protein V in the nucleus at early time points after adenovirus infection and conclude that protein V is able to enter the nucleus independently of the viral DNA/protein VII-complex (10). As an incoming virion protein present in the infected host-cell after entry into the host nucleus, protein V could have a yet unknown regulatory influence on establishing conditions favorable for the onset of viral replication. Furthermore, it is a late phase protein, which might not only be packed into new infectious particles, but also play a part in regulation of virion assembly. However, the last steps of adenoviral infections comprising assembly, encapsidation, maturation, escape of viral progeny and also the role of protein V during immediate early phase are still not understood in detail.

PML nuclear bodies (PML-NBs) are nuclear, spherical multi-protein complexes, located in the inter-chromosomal space, where they are tightly bound to the nuclear matrix (11). Many of the processes associated with PML-NBs are linked to a posttranslational modification (PTM) of the proteins involved, called SUMO. SUMO is short for small ubiquitin-like modifier, since it shares around 18% sequence similarity with ubiquitin and is covalently bound to its target proteins in a mechanistically comparable manner. In contrast to SUMO1, SUMO2/3 proteins are able to form polymeric chains, since they contain a conserved acceptor lysine residue within their sequence (12). The attachment of SUMO proteins to their targets occurs

136 in a reversible three-step enzymatic cascade. PML-NBs have been discussed as
137 nuclear sites for PTM themselves, and especially represent hotspots for SUMO
138 modification. All enzymes involved in SUMOylation or deSUMOylation of proteins
139 are present at the PML NBs and PML has been proposed to have an E3 SUMO ligase
140 activity (13).
141 Here, we show that protein V indeed represents a novel target of the host SUMO
142 machinery and partially localizes to PML nuclear domains. Remarkably, after
143 blocking protein V SUMOylation by site-directed mutagenesis, we see a beneficial
144 effect on viral gene expression and replication processes. Biochemical analyses
145 revealed that a block of protein V SUMO conjugation promotes viral DNA synthesis
146 and coordinates nucleoli association during productive infection.
147 Further functional studies of adenoviral structural proteins such as protein V
148 contribute to a profound understanding of the complex processes mentioned above,
149 and pave the way towards developing novel antiviral intervention strategies.

Materials and Methods

Cell lines and culture conditions.

H1299 (ATCC *Global Bioresource Center*, No. CRL-5803) and HeLa cells, 6His-SUMO1 Hela or 6His-SUMO2 Hela cells (kind gift from Ron T. Hay, University of Dundee, Scotland) stably expressing 6His-SUMO1 or 6His-SUMO2 (14) were grown in Dulbecco's modified Eagle's medium supplemented with 5% fetal calf serum, 100 U/ml penicillin and 100 µg/ml streptomycin in a 5% CO_2 atmosphere at 37°C. For HepaRG cells, the medium was supplemented with 10% fetal calf serum, 100 U/ml penicillin, 100 µg/ml streptomycin, 5 µg/ml of bovine insulin and 0.5 µM of hydrocortisone. 6His-SUMO HeLa cell lines were maintained under 2 µM puromycin selection. All cell lines were frequently tested for mycoplasma contamination.

Plasmids and transient transfections.

HA-V proteins were expressed from their respective cDNA under the control of the CMV immediate early promoter from pcDNA3 (Invitrogen) based vector plasmids. Flag-V proteins examined in this study were expressed from their respective cDNAs under the control of the CMV immediate early promotor from the pCMX3b vector plasmid. The expression plasmids were generated with oligonucleotide primers indicated in Table 1. Flag-V mutants were derived through single nucleotide exchanges by site-directed mutagenesis using the oligonucleotides shown in Table 1. For transient transfections, subconfluent cells were treated with a mixture of DNA and linear polyethylenimine (PEI, 25 kDa) as described before (15).

Viruses.

H5*pg*4100, which contains deletions in the E3-coding region, served as the wildtype (wt) HAdV-C5 virus (16). H5*pm*4242 carries four point mutations within the protein V coding sequence. It was derived by site-directed mutagenesis (16) using the oligo-nucleotide primers indicated in Table 1.

All viruses were propagated and titrated in H1299 cells. For this, infected cells were harvested 3-5 d p.i. and lysed by three freeze and thaw cycles. The supernatant containing HAdV was used to reinfect subconfluent H1299 cells. 24 h p.i. the concentration of infectious particles was determined by immunofluorescence staining of the adenoviral DNA binding protein E2A/DBP as described before in ffu/cell (17). HAdV were supplemented with 10 % sterile glycerol (v/v) to be preserved at -80°C. At 4°C, viral titers remain constant for several weeks.

Adenoviral progeny of infected cells was determined 24 h, 48 h and 72 h p.i. Cells harvested at these time points were stored at -20°C until samples were complete. Viral particles were released through repeated freeze and thaw cycles and subconfluent H1299 cells were reinfected with dilutions of the supernatants ranging from 10^{-2} to 10^{-4}. Viral titers were determined as described before as ffu/cell (18).

Antibodies and protein analysis.

Primary antibodies specific for viral proteins included E1B-55K mouse mAb 2A6 (19), E4orf6 mouse mAb RSA3 (20), L4-100K rat mAb 6B-10 (21), E2A-72K mouse mAb B6-8 (22), E1A mouse mAb M73 (23), E1B-19K rabbit pAb (24), HAdV-C5 rabbit polyclonal serum L133 (25), and protein V rabbit pAb (kindly provided by D. A. Matthews, University of Bristol, UK). Primary antibodies specific for cellular and

ectopically expressed proteins included anti-flag mouse mAb M2 (Sigma-Aldrich, Inc.), anti-HA-tag rat mAb 3F10 (Roche), anti-His-tag mouse mAb (Clontech), anti p53 mouse mAb Do-1 (Santa Cruz), anti B23 mouse mAb FC-61991 (Invitrogen) and ß-actin mouse mAb AC-15 (Sigma-Aldrich, Inc.). Secondary antibodies conjugated to horseradish peroxidase (HRP) for detection of proteins by immunoblotting were anti-rabbit IgG, anti-mouse IgG anti-rat IgG (Jackson/Dianova).

Protein extracts were prepared in RIPA lysis buffer (12) on ice for 30 min. Total-cell lysates were sonicated for 30 s (40 pulses, output 0.6, 0.8 impulses/s), before the cell debris was removed (11000 rpm, 3 min, 4°C). Protein concentration was determined photometrically with *Bradford Reagent* (BioRad). For Ni-NTA pull down, cells were harvested 48 h after treatment. 20 % of total cells were pelleted to determine steady-state protein concentrations as described above, whereas the remaining cells were resuspended in 5 ml guanidinium hydrochloride (GuHCl) lysis buffer (0.1 M Na_2HPO_4, 0.1 M NaH_2PO_4, 10 mM Tris/HCl pH 8.0, 20 mM Imidazole and 5 mM β-mercaptoethanol). Lysed cells in GuHCl were sonicated for 30 s (40 pulses, output 0.6, 0.8 impulses/s) and supplemented with 25 µl Ni-NTA agarose (Qiagen) prewashed with GuHCl. The samples were incubated over night at 4°C followed by centrifugation (4000 rpm, 10 min, 4°C). Sedimented agarose was washed once with buffer A (8 M urea, 0.1 M Na_2HPO_4, 0.1 M NaH_2PO_4, 10 mM Tris/HCl pH 8.0, 20 mM imidazole and 5 mM β-mercaptoethanol) and two times with buffer B (8 M urea, 0.1 M Na_2HPO_4, 0.1 M NaH_2PO_4, 10 mM Tris/HCl pH 6.3, 20 mM imidazole and 5 mM β -mercaptoethanol). 6His-SUMO conjugates were eluted from the Ni-NTA agarose with 30 µl Nickel resin elution buffer (200 mM imidazole, 5% (w/v) SDS, 150

mM Tris/HCl (pH 6.7), 30% (v/v) glycerol, 720 mM β-mercaptoethanol, 0.01% (w/v) bromophenol blue).

All protein samples were separated by SDS-PAGE after denaturation (SDS sample buffer (5x), 95°C, 3 min). Proteins were transferred to nitrocellulose blotting membranes (0.45 µm pore size) and visualized by immunoblotting (western blotting). The protein transfer was performed in a *Trans-Blot® Electrophoretic Transfer* Cell (BioRad, 'full wet' mode) in *Towbin* buffer (25 mM Tris/HCl (pH 8.3), 200 mM glycine, 0.05% (w/v) SDS, 20% (v/v) methanol) with 400 mA for 90 min. Membranes were incubated overnight at 4°C in phosphate-buffered saline (PBS) containing 5% nonfat dry milk. They were washed three times in PBS–0.1% Tween 20 (PBST) before they were incubated for 3 h with the appropriate primary antibody in PBST. Membranes were washed again three times in PBST before being incubated for 1 h with a secondary antibody conjugated to HRP (1:10000 in PBST, v/v) containing 3% nonfat dry milk. After washing three times in PBST, the bands were visualized by enhanced chemiluminescence (ECL) as recommended by the manufacturer (Pierce) on X-ray films (CEA RP). Autoradiograms were scanned and cropped using Adobe *Photoshop CS6*. Final figures were prepared using Adobe *Illustrator CS6* software.

Indirect immunofluorescence.

For indirect immunofluorescence, $2x10^5$ adherent, eukaryotic cells were seeded on sterile glass coverslips positioned in 6-well cell culture dishes. 24 hours later the cells were treated as experimentally required and at the time point of interest, all treated cells were fixed either with methanol at -20°C (10 min) or with paraformaldehyde (PFA, 4% (v/v) in PBS) at room temperature (20 min). If fixed with PFA, the cells had

to be permeabilized in phosphate-buffered saline (PBS) with 0.5 Triton X-100 for 10 min at room temperature prior to 10 min of blocking in Tris-buffered saline-BG (TBS-BG; BG represents 5% (w/v) BSA and 5% (w/v) glycine). Coverslips were treated for 30 min in a humidity chamber with the indicated primary antibody diluted in PBS. Afterwards, the cells were incubated 20 min with the corresponding secondary antibody diluted in PBS (Alexa 488® (Invitrogen)-, Cy3 (Jackson)-, FITC (Jackson)- or Texas red (Jackson)-conjugated secondary antibodies). Finally, nuclei were stained with dapi (4,6-diamidino-2-phenylindole) in PBS (1:1000, v/v) for 5 min, before the cells were mounted in glow medium (Energene). All steps were separated by 3 washing steps with PBS (5 min each). Dapi was rinsed off with double-distilled water. Digital images were acquired either with a confocal laser scanning microscope (Nikon) using the *NIS-Elements* software or with a wide field fluorescence microscope (Leica) using the *Leica Application Suite*. Images were processed with Adobe *Photoshop CS6* and assembled with *Adobe Illustrator CS6*. Colocalization analysis was calculated and visualized with *Fiji* (plugin: *Colocalization Threshold)*.

Isolation and quantification of nucleic acids.

To isolate RNA, cell samples ($4x10^6$ cells) in 600 µl *TRIzol*® (ThermoFisher) were incubated with 60 µl 1-bromo-3-chloropropane for 10 min at room temperature and centrifuged with 12000 g for 15 min at 4°C. Contained nucleic acids in the aqueous phase were precipitated with 500 µl isopropanol (12000 g, 10 min, 4°C), washed with 1 ml ethanol (75 %, v/v) by vortexing and pelleted (7500 g, 5 min, 4°C). The pellets were air-dried for 5-10 min and resuspended carefully in 80 µl RDD-buffer containing 10 µl RNase-free DNase I (Qiagen) to digest traces of remaining DNA for

30 min at room temperature. DNase I were heat inactivated (75 °C, 5 min) and RNAs were precipitated with RNase-free LiCl solution (Applied Biosystems, final concentration 2.5 M) for 30 min at -20°C. RNAs was pelleted with 16000 g for 20 min at 4°C washed with ice-cold ethanol (75 %, v/v). RNA pellets were air-dried for 5-10 min and dissolved for 10 min at 58°C in nucleic acid-free water (Promega).

Purified RNA was transcribed into complementary DNA (cDNA) by use of the *Reverse Transcription System* (Promega) according to the manufacturer's protocol. The reaction was primed with oligo (dT) primers to select for mRNAs. Transcribed cDNAs were stored at -20°C. All samples were additionally prepared without the reverse transcriptase to determine the level of background-DNA contamination during RT-PCR. No sample showed DNA concentrations higher than random background.

To isolate genomic DNA from cultured cells, collected cell pellets were resuspended in 200 µl of PBS (phosphate buffered saline) and supplemented with 20 µl of proteinase K (Sigma-Aldrich). All further steps have been performed according to the *QIAamp DNA Mini and Blood Mini Handbook* (Qiagen). Purified genomic DNA was dissolved 5 min in 200 µl of nucleic acid free-water (Promega) per sample and stored at -20°C.

Quantification of cDNA or genomic DNA was realized through real-time qPCR. Purified samples were diluted 1:100 with nucleic acid-free water (Promega) and 4.5 µl per sample were mixed with 5 µl *SensiMix Plus SYBR* (Quantace) and 0.5 µl of appropriate primer pairs (5 µM Primer-Mix, Table 1).

All primers used amplify a short fragment of 100-200 bp within a DNA coding sequence. The reaction was performed in a *Rotor-Gene 6000* (Corbett Life Sciences)

machine. Each sample was measured in technical duplicates to determine the average threshold cycle (CT). Levels of viral mRNA were calculated relative to cellular 18S rRNA, whereas genomic viral DNA was calculated relative to the cellular one-copy gene β2-microglobuline. Recording of the melting curves as well as agarose-gel electrophoreses of the RT-PCR products ensured the purity of samples/products. Obtained data was processed with the *Rotor-Gene Q 2.3.1* (Qiagen) software, calculations were done with Microsoft *Excel* and statistical analysis was performed in form of unpaired, two-tailed t-tests (GraphPad *Prism 5*). Graphs were generated in Prism 5 as well, whereas final figures were generated with Adobe *Illustrator CS6*.

Results

HAdV protein V partially colocalizes with host PML bodies. Protein V accumulates at the nucleoli of infected cells as well as diffusely in the nucleoplasm (7, 8). Our results confirm protein V proteins in the nuclei of infected cells (Fig. 1A). In 90 % of the analyzed cells (n = 40), protein V revealed nuclear accumulations (Fig. 1A, panels f, and j), colocalizing with nucleophosmin (B23), a cellular marker of nucleoli (26) (Fig. 1A, panels e, and i). By using the *Fiji* plugin *Colocalization Threshold*, analysis of pixel intensities within nucleolar regions and their direct surrounding resulted in a linear correlation of the red and green channel pixels with the gradient reflecting the ratio of their intensities (Fig. 1A, *right* panels). The plugin uses an auto threshold determination using the *Costes method* and the proportion of a signal in one channel that colocalizes with the signal in the other channel is reflected by the thresholded *Mander's correlation* coefficients (tM). The tM ranges from 0 to 1, where 0 means no colocalization and 1 means perfect colocalization of signal intensities. The tM values in Fig. 1A average the signal correlation in all nucleolar regions of one picture. This amounts to tM1 = 0.94 (green) and tM2 = 0.90 (red) for panels f-g and to tM1 = 0.87 (green) and tM2 = 0.88 (red) for panels j-k, respectively. Accordingly, accumulation of adenoviral protein V at the host nucleoli could be confirmed in HepaRG cells. Besides, we also found smaller nuclear protein V containing dots (Fig. 1A, panel f), indicating association with other host nuclear domains, such as PML-NBs.

We further elucidated whether this adenoviral core protein is conjugated with SUMO proteins. We transfected either flag- or HA-V expressing plasmid and observed an additional band between 55 and 70 kDa (Fig. 1B, left panel, lane 2), matching the size of a conjugated SUMO protein. Furthermore, a smear of flag-V protein towards

higher molecular weights was detected, which is typical for the formation of SUMO or ubiquitin chains. Similarly, HA-V shows discrete slower migrating bands, matching the size of poly SUMOylation (Fig. 1B, right panel, lane 2). An even faster migrating form was found at 35 kDa (Fig. 1B, right panel, lane 2), indicating an as yet unknown, C-terminally shortened isoform of HAdV protein V or protein degradation.

HAdV protein V is covalently modified with SUMO proteins. To validate protein V PTM SUMOylation, a flag-V expressing plasmid was transiently transfected into cells stably expressing 6His-tagged SUMO1 or 6His-tagged SUMO2 (12) prior to Ni-NTA purification (Fig. 2A). Our data show that SUMO2 chains are conjugated with the viral core protein V (Fig. 2A, left panel, lane 6). Additionally, the protein itself, migrating at a size of 50 kDa, is pulled down, indicating an unspecific interaction of a flag-V fraction with the Ni-NTA matrix (Fig. 2A, lanes 4 and 6). Modification of protein V with SUMO1 cannot be ruled out, since protein V expression is low compared to SUMO2 cells (Fig. 2A, right panel, lanes 4-6).

Next, we superinfected cells transiently expressing flag-V and analyzed SUMOylation of the viral core protein. Our result showes that protein V SUMOylation is weaker in 6His-SUMO2 HeLa cells with protein V expressed from the viral genome during infection compared to cells transiently overexpressing flag-V (Fig. 2B, left panel, lanes 6-8). However, 6His-SUMO2 HeLa cells superinfected and overexpressing flag-V reveal efficient protein V SUMOylation (Fig. 2B, lanes 6, and 8).

Identification of several putative protein V SCMs (*SUMO conjugation motifs*). Since we had observed protein V SUMO conjugation, we performed an *in silico* analysis of the viral protein to identify putative SUMO conjugation and/or SUMO interacting motifs (SIMs) (Fig. 3A). All algorithms used indicated three consensus SCM of high probability within V: K7, K23 and K162 (Fig. 3A, B; depicted in pink). Additionally, one nSCM (*non-consensus SUMO conjugation site*) was predicted with high probability at K24 and several nSCM with low or medium probabilities were found (Fig. 3A; depicted in green). Furthermore, three SIMs were predicted within protein V, although they have low probability and appear only with use of low thresholds (Fig. 3A; depicted in blue).

Based on these findings, different putative SCM mutants of HAdV protein V were generated by site-directed mutagenesis to determine the actual sites of protein V SUMOylation. The coding sequence of protein V was modified to substitute the lysine residue within the motif by arginine. This retains the local as well as the net charge of the protein and thereby reduces the possibility of conformational changes, which could cause a change or even a loss of function. To obtain those mutants, single nucleotides of the protein V coding sequence were exchanged by quick change PCR using the flag-V expression plasmid as a template. Since this results in a lysine to arginine exchange within the primary protein sequence of protein V (Fig. 3B; depicted in yellow), the mutants were named VK7R and VK162R. In the case of the third SCM, containing K23, the neighboring K24, which was predicted with low probability as a nSCM, was also substituted, leading to a double mutant named VK23/24R. Additional plasmids were generated with only one intact SCM left within

V (VK7/23/24R, VK23/24/162R and VK7/162R). V4xKR has alterations in all three SCM and the nSCM, containing K24 (Fig. 3B).

The influence of those SCM mutations on protein V SUMOylation was investigated in transfected HeLa or 6His-SUMO2 Hela cells, which were prepared for Ni-NTA purification 48 h p.t Intriguingly protein V4xKR showed severely reduced SUMO modification (Fig. 3C, lane 3). In contrast, the single SCM mutants, apart from protein VK7R, do not show such strong alteration of SUMO2 modification (Fig. 3C, left panel, lanes 4-6). The pattern of flag-protein VK23/24R is identical to that of flag-protein V (Fig. 3C, left panel, lanes 2 and 5), whereas flag-protein VK162R lacks certain bands (b and d), although the overall signal of the other bands is even stronger in comparison to the wt protein (Fig. 3C, left panel, lanes 2 and 6). Interestingly, flag-protein VK7R shows a reduction of SUMO2 modification almost as strong as protein V4xKR, although the amount of pulled down SUMO-conjugates is slightly higher than for protein V (Fig. 3C, left panel, lanes 2-4). This indicates a major role of lysine residue K7 for the SUMO conjugation with protein V. Noteworthy however, the input concentration of protein VK7R was reduced (Fig. 3C, left panel, lane 4). The protein V mutants with only one intact SCM were also compared to protein V wt and protein V4xKR (Fig. 3C, right panel). As a whole, the signal intensity of the Ni-NTA purification was stronger than in the previous experiment, leading to the occurrence of a new double band for flag-protein V at approximately 70 kDa (Fig. 3C, upper right panel, lane 2, band f). It can clearly be assigned to K162, since it is not visible if this residue is substituted by arginine (Fig. 3C, right panel, lanes 2-6). The same is true for SUMO band d (Fig. 3C, right panel, lanes 4-6), which matches the result of the previous experiment (Fig. 3C, left panel,

lanes 4-6). In contrast to the previous experiment, it does not make a difference whether K7 or K23/24 were exchanged. If one site is still intact, the pattern of SUMO2 modification is identical (Fig. 3C, right panel, lanes 4-5). Hence, the residues seem to be able to compensate for the lack of each other, indicating that the drastic reduction of protein VK7R SUMOylation (Fig. 3C, left panel, lanes 2-4) rather results from its low protein concentration. If both conjugation sites are missing and only SCM K162 is present, band c disappears (Fig. 3C, right panel, lane 6). Additionally, bands a, e and g are less intense, indicating a greater dependence of these SUMO signals on K7, K23 and K24 than K162 (Fig. 3C, right panel, lanes 3-6). Band b is not clearly visible in all of the protein V-SCM mutants (Fig. 3C, right panel, lanes 3-6). The combination of these observations results in the SUMO2 pattern of protein V4xKR where four SUMO bands (b-d and f) are no longer detectable and the others are reduced (Fig. 3C, left panel, lanes 2-3). Taken together, only two bands of the protein V SUMO2 pattern can be precisely assigned to a certain SCM, i.e. d and f belonging to K162. Remarkably, protein V still shows SUMO2 modification if all its SCM are altered, although significantly reduced (Fig. 3C, lane 3). These results point to the fact that HAdV protein V is modified with SUMO proteins not only at one, but at different SCM, and that even further nSCM must be involved.

Reduced protein V SUMO conjugation alters the subcellular distribution of the viral protein. To elucidate whether SUMO conjugation with protein V changes its localization in distinct fractions within the nucleus, we analyzed immunofluorescence of the wt protein and the SCM mutants in 6His-SUMO2 HeLa cells (Fig. 4). A stable expression of SUMO2 was chosen to emphasize the difference

421 between wt protein V and its SCM mutants. As expected, the most abundant
422 phenotype of flag-V shows clear accumulations in the nucleus and a weak diffuse
423 signal in the nucleoplasm (Fig. 4A, panels d-e, pie charts). A similar distribution was
424 observed for the single SCM mutant flag-VK7R (Fig. 4B, panels j-k). In the case of
425 flag-VK23/24R, flag-VK162R, flag-VK7/23/24R and flag-VK23/24/162R the
426 percentage of diffuse protein-signal increased (Fig. 4B, panels m-t, y-z), whereas flag-
427 V4xKR transfected cells show distinct nucleolar accumulations only with a maximum
428 of 40% (Fig. 4A, panels g-h, pie charts). Although the accumulations remain visible in
429 the majority of transfected cells, they are often blurry and merge with the diffuse
430 fraction of protein V in the nucleoplasm. This type of subcellular distribution was
431 also detected in the majority of 6His-SUMO2 Hela cells positive for flag-VK7/162R
432 (Fig. 4AB, panels v-z). The amount of cells showing distinct protein V accumulations
433 at the nucleoli depends on the cell line and ranges from approximately 60-90% (Fig.
434 4C). Overall, these findings indicate that the lack of certain SCM within protein V
435 leads to reduced accumulation of the protein at the host nucleoli. A significant effect,
436 however, cannot be assigned to specific lysine residues, but depends on the
437 combined absence of at least all three SCM within protein V.
438
439 **Protein V SCMs affect virus gene expression and replication.** To elucidate the role
440 of this protein V SUMOylation during the course of adenoviral infection, a mutant
441 virus was generated where the lysine residues K7, K23 and K162 of the SCM as well
442 as K24, being part of a neighboring nSCM, are substituted by an arginine R, as before
443 in the mutant flag-V4xKR (Fig. 5A, B). We investigated the SUMOylation of protein
444 V during wt (H5*pg*4100) and mutant virus (H5*pm*4242) infection assays in 6His-

SUMO2-expressing HeLa cells (Fig. 5C). Total-cell lysates were subsequently purified 24 h p.i. with a Ni-NTA matrix to pull down 6His-SUMO2 conjugates. Pull down of protein V from mutant virus-infected cells shows a SUMO2 ladder with severely reduced signal intensities, compared to protein V from wt infected cells (Fig. 5C, left panel, lanes 2-3). As observed in the transient transfection experiments (Fig. 3), protein V SUMO bands a, c, e and f are severly reduced in protein V SCM mutant virus infected cells, whereas bands b and d are already very weak in wt infected cells (Fig. 5C, left panel, lanes 2-3).

To validate viral replication, we monitored adenoviral progeny production in protein V SCM mutant virus infected HepaRG cells compared to wt particle synthesis (Fig. 6A). An average of three independent experiments amounted to an approximately 2.5-fold increase in viral progeny produced 24 h p.i. in mutant virus infected cells (Fig. 6A). This increase over HAdV wt declines within 72 h p.i., but the ratio remains greater than 1.

The tendency of the mutant virus to produce more infectious particles was also reflected by the equilibrium concentrations of different adenoviral proteins, assessed in an additional time course experiment (Fig. 6B). Early adenoviral proteins E1A, E1B-19K and E1B-55K appeared 8 h earlier during protein V SCM mutant virus infection than in HAdV wt infected cells (Fig. 6B, lanes 2-4 and 7-9). The gene products E2A and E4orf6 were present in higher concentrations at corresponding time points (Fig. 6B, lanes 3-4 and 8-9). Similarly, the late protein L4-100K occurred earlier in cells infected with the protein V SCM mutant virus (Fig. 6B, lanes 4 and 8) and many of the capsid proteins showed a stronger signal than in wt infected cells (Fig. 6B, lanes 5-6 and 9-11). Only the mutated protein V is less abundant during

HAdV protein V SCM mutant infection (Fig. 6B, lanes 5-6 and 10-11). Furthermore, levels of the cellular tumor suppressor p53 decrease more efficiently during mutant virus infection (Fig. 6B, lanes 4-6 and 9-11). In conclusion, the HAdV protein V SCM mutant replication cycle is accelerated in comparison with wt virus.

To monitor viral transcription, cells were infected either with HAdV wt or with the protein V SCM mutant virus and harvested 6, 12 or 24 h p.i. Total RNA was isolated and mRNAs were reverse transcribed. The resulting cDNA was amplified by RT-PCR with primer pairs matching different regions of the adenoviral genome to reveal the relationship between early as well as late mRNAs in the differently infected HepaRG cells. As with the previous time course experiments at the protein level, all viral mRNAs investigated were synthesized earlier or with enhanced concentrations at particular time points in protein V SCM mutant virus infected cells (Fig. 6C). Interestingly, E1A-mRNA concentrations were already ~ two-fold higher at the early time points 6 and 12 h p.i. This observation was similar for the early viral mRNAs encoding E1B-55K and E4orf6, albeit they were only detected in protein V SCM mutant virus infected cells at the earliest time point measured, 6 h p.i. (data not shown). The elevated mRNA concentrations of E2A were even more pronounced. Already 6 h p.i. an approximately 12.5-fold excess of E2A-mRNA could be detected, which declined later on, as also found for the other viral mRNAs (Fig. 6C).

Comparable to adenoviral protein analysis, also late viral mRNAs were influenced (Fig. 6C). Interestingly, not only hexon mRNA, but also protein V mRNA already occurred 12 h after protein V SCM mutant virus infection, whereas it cannot be detected earlier than 24 h after HAdV wt infection. However, protein V SCM was the only protein with reduced steady state concentrations in the protein time course

493 experiment (Fig. 6B). Taken together, these results further underline an enhanced
494 efficacy of the HAdV protein V SCM mutant virus early during infection, which
495 occurs prior to translation of adenoviral proteins.
496 To substantiate our data, we repeated virus yield (Fig. 6D) and protein synthesis (Fig.
497 6D) in another human cell line. Our data showed that also in H1299 cells, adenoviral
498 progeny production in protein V SCM mutant virus infected cells was more efficient
499 than after wt infection (Fig. 6D). In accordance with the results obtained in HepaRG
500 cells, the mutant virus produces enhanced levels of early viral proteins, assessed in
501 an additional time course experiment (Fig. 6E).
502
503 **Protein V SUMOylation promotes nucleoli association of the viral factor.** To reveal
504 the effect of protein V mutations on subcellular protein distribution during
505 productive infection, cells infected with HAdV wt or the protein V SCM mutant
506 virus were prepared for immunofluorescence analysis 24 h p.i. The cells were double
507 stained for protein V and either E1A (Fig. 7A), E1B-55K (Fig. 7B) or E2A (Fig. 7C),
508 regulatory adenoviral proteins showing higher concentrations at early time points
509 during protein V SCM mutant virus infection (Fig. 6B). E1A was diffusely distributed
510 throughout the whole nucleus of infected cells except the nucleoli (Fig. 7A, panels g,
511 and k). E1B-55K accumulated in speckled fractions of different size and shape within
512 the cytoplasm, and showed an additional diffuse signal in the nucleus (Fig. 7B,
513 panels g, and k). Consequently, none of the two proteins showed a noticable
514 colocalization with protein V at the nucleoli. Only parts of their diffuse fractions
515 overlap with diffuse portions of protein V (Fig. 7A and 7B, panels e and ,i). E2A
516 forms spherical structures within the nucleus, which are known to be the sites of

517 viral replication. They varied from small filled dots to huge hollow spheres, in both,
518 cells infected with HAdV wt or the protein V SCM mutant virus (Fig. 7C, panels g,
519 and k). Hence, no difference in the localization of essential early viral proteins can be
520 detected between HAdV wt and protein V SCM mutant virus-infected HepaRG cells.
521 Furthermore, the sites of viral replication and the host nucleoli where protein V
522 accumulates, exclude each other. This leads to separate fractions of protein V and
523 E2A during wildtype infection, apart from the diffuse portion of protein V (Fig. 7C,
524 panel e) (11). This finding was confirmed in a colocalization study of panels f-g
525 where the thresholded *Mander's split coefficients* resulted in tM1 = 0.24 for the red
526 channel (protein V) and tM2 = 0.54 for the green channel (E2A). This phenomenon
527 was less pronounced in 42% of protein V SCM mutant virus infected HepaRG cells (n
528 = 12), where some portion of protein V accumulated in small dots at the periphery of
529 the nucleus, close to the nuclear membrane (Fig. 7C, panel j). According to the
530 intensity overlay of red and green channels in the nuclear area these spherical
531 structures indeed colocalize with corresponding dots of E2A, leading to a grey signal
532 (Fig. 7C, lower right panel). On the contrary, the green intensity corresponding to
533 E2A clearly dominates the red signal in wildtype infected cell nuclei (Fig. 7C, upper
534 right panel). In protein V SCM mutant virus infected cells, E2A signal intensities
535 colocalize with those of protein V (tM2 = 0.85) and a greater nuclear portion of
536 protein V correlates with E2A signals (tM1 = 0.48) than in wildtype infected cells
537 (tM1 = 0.24).
538 In addition, V4xKR accumulated less clearly within the nucleus than protein V wt
539 (Fig. 7A - 7D). An average of four independent immunofluorescence analyses where
540 protein V was stained, yielded 73 % of HAdV wt infected cells where protein V

clearly accumulates at host nucleoli. In contrast, this phenotype was only seen in 42 % of HepaRG cells infected with the protein V SCM mutant virus (Fig. 7E). This tendency of protein V SCM being more diffusely distributed in the host nucleus was also seen in each individual experiment (see representatively Fig. 7A-C, panels f, and j), although the experimental conditions differed slightly (Fig. 7D). In conclusion, the lack of SCM within HAdV protein V reduces the ability of the protein to accumulate at the host nucleoli.

Reduction of protein V SUMOylation promotes viral DNA replication. As a consequence of earlier viral protein expression during HAdV protein V SCM mutant virus infection compared to wt infection, it was expected that the onset of viral DNA-replication might be accelerated as well. To test this hypothesis, HepaRG cells were infected either with the protein V SCM mutant or with the wt virus and harvested 1, 16, 24 and 48 h p.i.. The genomic DNA of collected samples was isolated, purified and analyzed by PCR. At each time point, the HAdV DNA was determined relative to the one-copy gene β2-microglobuline to avoid false differences due to varying DNA contents of the samples. This approach indeed confirmed accelerated viral DNA replication during protein V SCM mutant virus infection (Fig. 8), showing its greatest advantage 16 h p.i. (Fig. 8B), shortly after the onset of viral DNA replication. This difference decreases with proceeding infection and levels out two days after infection (Fig. 8). Interestingly, already 1 h p.i. more viral DNA was isolated from mutant virus infected HepaRG cells compared to those infected with HAdV wt in four independent experiments, indicating some additional effect on virus entry processes (Fig. 8).

Discussion

Here, we report that disrupting protein V consensus SUMO conjugation motifs (SCM) by site directed mutagenesis results in a global acceleration of viral replication and progeny production. Mutation of the three SCM within HAdV protein V causes a loss of distinct SUMO signals and an overall intensity reduction of the remaining ones. This significant reduction of protein V SUMOylation during mutant virus infection could be partially caused by lower amounts of the protein compared to HAdV wt infection. However, the loss of signal intensity is more pronounced for certain SUMO signals, which could refer to mono-or polyubiquitinylation. The lack of protein V SCM reduced SUMOylation of the protein during transient transfection studies as well as during HAdV infection. Hence, the loss of certain SUMO signals is apparently the actual cause of the observed accelerated viral life cycle. This would be an interesting phenotype, since it matches the emerging hypothesis of SUMOylation dependent regulation of proteins involved in intrinsic and innate immunity (27). However, this raises the question why the virus would evolve SUMO conjugation sites in protein V if this is detrimental for efficient infection. Our observations suggest that it might represent a bottleneck for the virus to process enhanced replication fitness, as adenoviruses need to not kill the host before spread of infection.

PML bodies represent SUMOylation hotspots of the cell. The interplay of viruses with infected host cells is influenced by SUMOylation of both viral and cellular proteins (28, 29). Hence, the SUMOylation of proteins has emerged as one key post-translational modification (PTM). SUMO proteins, which belong to the family of ubiquitin-like modifiers (UBLs), can be covalently bound to target proteins or non-

589 covalently interact with SIM motifs of other proteins to affect their function. It is
590 widely assumed that PML nuclear bodies are needed to concentrate proteins in a
591 defined area to increase reaction efficiencies and facilitate their regulation. Here, we
592 observe that there are different protein V fractions in the infected host nucleus. Next
593 to its known localization at host nucleoli, we find a large protein V portion
594 distributed over the whole nucleoplasm and also a partial colocalization of HAdV
595 protein V with PML. However, these aggregates no longer have their typical size and
596 shape. They appear larger in size and often localize in proximity to the nuclear
597 envelope. We were unable to detect protein V interaction with any constituent PML-
598 NB factor, i.e. PML, Sp100 or Daxx. However, since the composition of PML-NBs is
599 dynamic, a temporary interaction with specific host determinants of the PML-NBs
600 remains possible.
601
602 Interestingly, the equilibrium of early viral protein concentrations were already
603 elevated during infection with the HAdV protein V SCM mutant (H5*pm*4242).
604 However, newly translated protein V, lacking its SCM, cannot be the cause of this
605 phenotype, since it is only expressed in the late phase of adenoviral infection. This
606 points to incoming modified protein V having an influence on early viral protein
607 levels. In accordance with this hypothesis, adenoviral mRNA concentrations are also
608 already influenced at a time point where viral transcription has just started and only
609 incoming virion proteins of HAdV can be present. This is especially striking in case
610 of E1A mRNA, since it is known to be the first adenoviral protein expressed.
611 Whether viral transcription is influenced directly or whether the viral mRNAs might

612 rather be stabilized post-transcriptionally, remains to be clarified in future
613 experiments.
614 So far, protein V has not been identified as RNA-binding protein (RBP). Moreover,
615 alignment of its primary structure with known RNA-recognition motifs (RRM), zinc
616 fingers or the KH-domain (30) identified no matches
617 (https://blast.ncbi.nlm.nih.gov/Blast.cgi?PROGRAM=blastp&PAGE_TYPE=BlastSe
618 arch&LINK_LOC=blasthome), although protein V could act on RNA in a complex
619 with other cellular or even viral RBPs.
620 Another explanation for the accelerated protein V SCM mutant virus phenotype
621 could relate to viral entry and nuclear uptake of the viral core. This possibility was
622 supported by monitoring viral DNA replication, where already 1 h p.i. more viral
623 DNA could be detected in protein V SCM mutant virus infected cells.
624 Immunoblotting of proteins originating from three different infected cell lines
625 revealed that protein V SCM occurs in lower steady state concentrations than wt
626 protein V (data not shown). However, protein V mRNA expression is accelerated
627 during protein V SCM mutant virus infection, just like all the adenoviral mRNAs
628 investigated. Some reasons for lower mutant protein V levels could be lower protein
629 stability, relocalization of protein V SCM to insoluble fractions such as the nuclear
630 matrix or even degradation of the protein. However, the latter possibility seems
631 unlikely, since protein V protein concentration increased over time.
632 SUMO conjugation to a protein is linked to increased protein stability, because
633 competitive ubiquitinylation is prevented at the corresponding lysine residue, and
634 polyubiquitination represents a signal for proteasomal degradation. However,
635 protein V SCM stability would not be affected by increasing ubiquitinylation, since

636 the corresponding lysine residues were substituted by arginine. However, these
637 amino acid substitutions at four individual positions in protein V, could affect the
638 protein conformation and thereby its stability, function or both. To minimize the
639 probability of such an unwanted side effects, arginine was specifically chosen as a
640 substitute for lysine, since it retains the local and net charge of the altered protein. In
641 addition, the effect of these point mutations on structural elements of HAdV protein
642 V was evaluated by *I-TASSER* (*Iterative Threading ASSEmbly Refinement*). Since no
643 change in any secondary structure element was seen, and the accuracy of tertiary
644 structure predictions was weak, the probability of structural changes within protein
645 V was assessed as low.
646 Notably, HAdV protein V has been predicted to be a protein of low structural order
647 by different algorithms *APSSP 2* (*Advanced Protein Secondary Structure Prediction*
648 *Server*), *PSIPRED V3.3* and *I-TASSER*. Intrinsically disordered proteins (IDPs) often
649 contain a combination of disordered regions (IDRs) and structured domains, as was
650 predicted for HAdV protein V. The high degree of disorder results in high protein
651 flexibility, allowing for dynamic switching between conformations. This allows IDPs
652 to interact with a variety of different target molecules, such as DNA, other proteins,
653 complexes or PTMs. Upon binding to different targets many IDPs form well-defined
654 induced-fit structures that depend on the binding partner (31, 32). For instance,
655 binding of HAdV protein V to DNA in solution was shown to be sequence
656 independent, mainly depending on the soluble N-terminus of the protein (aa 1-200)
657 (3, 6, 33). However, inside adenoviral virions fewer regions of protein V contact the
658 viral genome, indicating that DNA binding regions are masked sterically or through

interactions with other viral proteins, and this results in a higher order complex that is destabilized during capsid disassembly (6).

Possibly, HAdV protein V, lacking its SCM, could change its behavior within mature adenoviral particles and thereby affect their stability. A pre-weakening of adenoviral virions might facilitate viral uptake and disassembly, which starts already at the cell surface (34). If the presence of less protein V is the cause of reduced protein V signals after immunoblotting of protein V SCM mutant virus infected cells, also a lack of protein V incorporation into new infectious particles would be imaginable. Only a few studies investigating posttranslational modifications within viral particles have been published so far. A very early one in the 1980s revealed the presence of phosphorylated, adenoviral proteins. Indeed, phosphorylated protein IIIa could be found in mature particles, whereas protein V phosphorylation disappeared during virion maturation (35). However, other PTMs of adenoviral proteins within viral particles have never been reported. Very recently, it could be shown that the major core protein VII is acetylated at specific sites, but only in cell extracts and not within purified viruses (36). The possibility remains that a change in protein V SUMOylation already influences the stability within adenoviral virions and facilitates their uptake into host cells.

The hypothesis of adenoviral protein V being a strictly regulated protein fits the finding that protein V is necessary for viral progeny production. An HAdV mutant virus, depleted of protein V, could only be rescued through the coding region of protein μ acquiring three additional point mutations. Otherwise, the production of infectious progeny failed (37). In addition, there is evidence that nucleoplasmatic nucleophosmin (B23.1, NPM1) is required for efficient adenoviral replication (38)

683 (39). NPM1 is a nucleolar phosphoprotein, which is only modestly expressed in
684 human primary cells. In contrast, it is overexpressed in various types of human
685 tumors (40) where it is localized in the nucleoli as well as in the nucleoplasm (41).
686 The SCM mutation within the coding sequence of HAdV protein V leads to a
687 decrease of the overall protein signal after immunoblotting as well as in
688 immunofluorescence analysis of infected cells, compared to cells infected with HAdV
689 wildtype. However, not only the amounts of detected protein V differ between viral
690 infections; protein V, lacking its SCM, seems to have a reduced affinity to accumulate
691 at host nucleoli. Transfection experiments further revealed that the mutation of
692 single SCM within HAdV protein V does not have a significant impact on the
693 localization of the protein in different cell lines. Only if all three SCM are altered,
694 protein V accumulations are significantly less pronounced. This indicates that the
695 SUMOylated protein V is preferentially directed to nucleoli.
696 In conclusion our findings show that protein V SUMO modification negatively
697 regulates the HAdV life cycle and might represent a novel antiviral target structure
698 for therapy approaches. Conversely, blocking SUMO conjugation to HAdV protein V
699 protein could potentially impact gene vector development and efficacy during
700 production.

Acknowledgements

We greatly appreciate the critical comments and scientific discussion from Nicole Fischer (University Hospital Hamburg Eppendorf, Germany) and Ron T. Hay (University of Dundee, Scotland). Moreover, we want to thank David Matthews (University of Bristol, UK) for providing the protein V specific antibody and Ron T. Hay (University of Dundee, Scotland) for the Hela SUMO cell lines.

SS and NF were supported by *Deutsche Krebsforschung e.V.*. Part of this work was supported by the *Deutsche Forschungsgemeinschaft DFG (SFB TRR179)*, *Else Kröner-Fresenius-Stiftung*, *Dräger Stiftung e. V*. and the *B. Braun Stiftung*. The Heinrich Pette Institute, Leibniz Institute for Experimental Virology is supported by the *Freie und Hansestadt Hamburg* and the *Bundesministerium für Gesundheit* (BMG).

References

1. **Berk AJ.** 2005. Recent lessons in gene expression, cell cycle control, and cell biology from adenovirus. Oncogene **24:**7673-7685.
2. **Lion T.** 2014. Adenovirus infections in immunocompetent and immunocompromised patients. Clin Microbiol Rev **27:**441-462.
3. **Chatterjee PK, Vayda ME, Flint SJ.** 1985. Interactions among the three adenovirus core proteins. J Virol **55:**379-386.
4. **Alestrom P, Akusjarvi G, Lager M, Yeh-kai L, Pettersson U.** 1984. Genes encoding the core proteins of adenovirus type 2. J Biol Chem **259:**13980-13985.
5. **Davison AJ, Benko M, Harrach B.** 2003. Genetic content and evolution of adenoviruses. J Gen Virol **84:**2895-2908.
6. **Perez-Vargas J, Vaughan RC, Houser C, Hastie KM, Kao CC, Nemerow GR.** 2014. Isolation and characterization of the DNA and protein binding activities of adenovirus core protein V. J Virol **88:**9287-9296.
7. **Matthews DA.** 2001. Adenovirus protein V induces redistribution of nucleolin and B23 from nucleolus to cytoplasm. J Virol **75:**1031-1038.
8. **Matthews DA, Russell WC.** 1998. Adenovirus core protein V is delivered by the invading virus to the nucleus of the infected cell and later in infection is associated with nucleoli. J Gen Virol **79 (Pt 7):**1671-1675.
9. **Puntener D, Engelke MF, Ruzsics Z, Strunze S, Wilhelm C, Greber UF.** 2011. Stepwise loss of fluorescent core protein V from human adenovirus during entry into cells. J Virol **85:**481-496.
10. **Hindley CE, Lawrence FJ, Matthews DA.** 2007. A role for transportin in the nuclear import of adenovirus core proteins and DNA. Traffic **8:**1313-1322.
11. **Bernardi R, Pandolfi PP.** 2007. Structure, dynamics and functions of promyelocytic leukaemia nuclear bodies. Nat Rev Mol Cell Biol **8:**1006-1016.
12. **Tatham MH, Jaffray E, Vaughan OA, Desterro JM, Botting CH, Naismith JH, Hay RT.** 2001. Polymeric chains of SUMO-2 and SUMO-3 are conjugated to protein substrates by SAE1/SAE2 and UBC9. J Biol Chem **276:**35368-35374.
13. **Chu Y, Yang X.** 2011. SUMO E3 ligase activity of TRIM proteins. Oncogene **30:**1108-1116.
14. **Tatham MH, Rodriguez MS, Xirodimas DP, Hay RT.** 2009. Detection of protein SUMOylation in vivo. Nat Protoc **4:**1363-1371.
15. **Wimmer P, Berscheminski J, Blanchette P, Groitl P, Branton PE, Hay RT, Dobner T, Schreiner S.** 2015. PML isoforms IV and V contribute to adenovirus-mediated oncogenic transformation by functionally inhibiting the tumor-suppressor p53. Oncogene doi:10.1038/onc.2015.63.
16. **Groitl P, Dobner T.** 2007. Construction of adenovirus type 5 early region 1 and 4 virus mutants. Methods Mol Med **130:**29-39.
17. **Burck C, Mund A, Berscheminski J, Kieweg L, Muncheberg S, Dobner T, Schreiner S.** 2015. KAP1 Is a Host Restriction Factor That Promotes Human Adenovirus E1B-55K SUMO Modification. J Virol **90:**930-946.
18. **Schreiner S, Bürck C, Glass M, Groitl P, Wimmer P, Kinkley S, Mund A, Everett RD, Dobner T.** 2013. Control of Human Adenovirus type 5 (Ad5) gene expression by cellular Daxx/ATRX chromatin-associated complexes. Nucleic Acids Res **41:**3532-3550.

19. **Sarnow P, Hearing P, Anderson CW, Reich N, Levine AJ.** 1982. Identification and characterization of an immunologically conserved adenovirus early region 11,000 Mr protein and its association with the nuclear matrix. J Mol Biol **162:**565-583.
20. **Marton MJ, Baim SB, Ornelles DA, Shenk T.** 1990. The adenovirus E4 17-kilodalton protein complexes with the cellular transcription factor E2F, altering its DNA-binding properties and stimulating E1A-independent accumulation of E2 mRNA. J Virol **64:**2345-2359.
21. **Kzhyshkowska J, Kremmer E, Hofmann M, Wolf H, Dobner T.** 2004. Protein arginine methylation during lytic adenovirus infection. Biochem J **383:**259-265.
22. **Reich NC, Sarnow P, Duprey E, Levine AJ.** 1983. Monoclonal antibodies which recognize native and denatured forms of the adenovirus DNA-binding protein. Virology **128:**480-484.
23. **Harlow E, Franza BR, Jr., Schley C.** 1985. Monoclonal antibodies specific for adenovirus early region 1A proteins: extensive heterogeneity in early region 1A products. J Virol **55:**533-546.
24. **Lomonosova E, Subramanian T, Chinnadurai G.** 2005. Mitochondrial localization of p53 during adenovirus infection and regulation of its activity by E1B-19K. Oncogene **24:**6796-6808.
25. **Kindsmüller K, Groitl P, Härtl B, Blanchette P, Hauber J, Dobner T.** 2007. Intranuclear targeting and nuclear export of the adenovirus E1B-55K protein are regulated by SUMO1 conjugation. Proc Natl Acad Sci USA **104:**6684-6689.
26. **Spector DL, Ochs RL, Busch H.** 1984. Silver staining, immunofluorescence, and immunoelectron microscopic localization of nucleolar phosphoproteins B23 and C23. Chromosoma **90:**139-148.
27. **Hannoun Z, Maarifi G, Chelbi-Alix MK.** 2016. The implication of SUMO in intrinsic and innate immunity. Cytokine Growth Factor Rev **29:**3-16.
28. **Wimmer P, Schreiner S.** 2015. Viral Mimicry to Usurp Ubiquitin and SUMO Host Pathways. Viruses **7:**4854-4872.
29. **Wimmer P, Schreiner S, Dobner T.** 2012. Human pathogens and the host cell SUMOylation system. J Virol **86:**642-654.
30. **Stefl R, Skrisovska L, Allain FH.** 2005. RNA sequence- and shape-dependent recognition by proteins in the ribonucleoprotein particle. EMBO Rep **6:**33-38.
31. **Berlow RB, Dyson HJ, Wright PE.** 2015. Functional advantages of dynamic protein disorder. FEBS Lett **589:**2433-2440.
32. **Wright PE, Dyson HJ.** 2015. Intrinsically disordered proteins in cellular signalling and regulation. Nat Rev Mol Cell Biol **16:**18-29.
33. **Chatterjee PK, Vayda ME, Flint SJ.** 1986. Identification of proteins and protein domains that contact DNA within adenovirus nucleoprotein cores by ultraviolet light crosslinking of oligonucleotides 32P-labelled in vivo. J Mol Biol **188:**23-37.
34. **Suomalainen M, Greber UF.** 2013. Uncoating of non-enveloped viruses. Curr Opin Virol **3:**27-33.
35. **Weber JM, Khittoo G.** 1983. The role of phosphorylation and core protein V in adenovirus assembly. J Gen Virol **64 (Pt 9):**2063-2068.
36. **Avgousti DC, Herrmann C, Kulej K, Pancholi NJ, Sekulic N, Petrescu J, Molden RC, Blumenthal D, Paris AJ, Reyes ED, Ostapchuk P, Hearing P,**

Seeholzer SH, Worthen GS, Black BE, Garcia BA, Weitzman MD. 2016. A core viral protein binds host nucleosomes to sequester immune danger signals. Nature **535:**173-177.

37. **Ugai H, Borovjagin AV, Le LP, Wang M, Curiel DT.** 2007. Thermostability/infectivity defect caused by deletion of the core protein V gene in human adenovirus type 5 is rescued by thermo-selectable mutations in the core protein X precursor. J Mol Biol **366:**1142-1160.

38. **Ugai H, Dobbins GC, Wang M, Le LP, Matthews DA, Curiel DT.** 2012. Adenoviral protein V promotes a process of viral assembly through nucleophosmin 1. Virology **432:**283-295.

39. **Samad MA, Komatsu T, Okuwaki M, Nagata K.** 2012. B23/nucleophosmin is involved in regulation of adenovirus chromatin structure at late infection stages, but not in virus replication and transcription. J Gen Virol **93:**1328-1338.

40. **Grisendi S, Mecucci C, Falini B, Pandolfi PP.** 2006. Nucleophosmin and cancer. Nat Rev Cancer **6:**493-505.

41. **Subong EN, Shue MJ, Epstein JI, Briggman JV, Chan PK, Partin AW.** 1999. Monoclonal antibody to prostate cancer nuclear matrix protein (PRO:4-216) recognizes nucleophosmin/B23. Prostate **39:**298-304.

824 **Tables**

825

826 **Table 1**

Primer description	Primer sequence
18S rRNA	5′- CGGCTACCACATCCAAGGAA -3′
Flag-V	5′- GCTGGAATTACCGCGGCT -3′
Flag-VK7R	5′-ACAGGATCCTCCAAGCGCAAAATCAAAGAAGAGATGC-3′; 5′-ACAGAATTCTTAAACGATGCTGGGGTGGTAGCG-3′
Flag-VK23/24R	5′-CCAAGCGCAAAATCAGAGAAGAGATGCTCC-3′ 5′-GGAGCATCTCTTCTCTGATTTTGCGCTTGG-3′
Flag-V K162R	5′-CTATGGCCCCCCGAGGAGGGAAGAGCAGGATTA C-3′ 5′-GTAATCCTGCTCTTCCCTCCTCGGGGGGCCATAG-3′
E1A	5′-CCAAGCGCAAAATCAGAGAAGAGATGCTCC-3′ 5′-CACCAGACTCGCGCCTTAGGCCGCGCTTTT-3′
E2A	5′-GTG CCC CAT TAA ACC AGT TG-3′ 5′-GGC GTT TAC AGC TCA AGT CC-3′
protein V	5′-GAA ATT ACG GTG ATG AAC CCG-3′ 5′-CAG CCT CCA TGC CCT TCT CC-3′
hexon	5′-CCC GAA AGC TAA AGC GGG TC-3′ 5′-CGT AAA GAC TAC GGT GGT GC-3′
β2-microglobuline	5′-CGC TGG ACA TGA CTT TTG AG-3′ 5′-GAA CGG TGT GCG CAG GTA-3′ 5′-TGA GTA TGC CTG CCG TGT GA-3′ 5′-CCA TGT GAC TTT GTC ACA GCC CAA GAT AGT T-3′

827

828

Figure Legends

Figure 1. HAdV protein V association with host PML structures. (**A**) HepaRG cells were infected with H5*pg*4100 (moi 20) and fixed with 4% PFA 24 h p.i. Mock means uninfected control. Proteins were detected with pab α- protein V and mab FC-61991 (α-B23). Primary antibodies were detected with Alexa488- (green) or Cy3- (red) conjugated secondary antibodies and nuclei were stained with dapi (blue). *Merge* indicates the overlay of single images of each row. Images were captured with a Nikon confocal fluorescence microscope. Colocalization of adenoviral protein V and B23 at host nucleoli is depicted on the *right* by 2D-histograms, which are correlating the pixel intensities of two channels and show the corresponding channel overlay of the analyzed regions of interest (ROI). tM means thresholded Mander's split coefficient where the number indicates the channel, 1 corresponds to the red channel (B23) and 2 corresponds to the green channel (protein V). (**B**) HepaRG cells were transfected with either 10 µg of empty vector control, pCMX3b-flag-V expression plasmid (left panel) or pcDNA3-HA-V expression plasmid. Cells were harvested 48 h p.t.. Total-cell lysates were resolved by SDS-PAGE and visualized by immunoblotting. Levels of flag-V and HA-V were detected by using mab M2 (α-flag) and mab 3F10 (α-HA), input levels of β-actin were detected by using mab AC-15 (α-β-actin). Molecular weights in kDa are indicated on the left, while corresponding proteins are labeled on the right.

Figure 2. Protein V is a novel SUMO target in the host cell. (**A**) HeLa cells and HeLa cells stably expressing 6His-SUMO1 or 6His-SUMO2 were transfected with 10 µg of an empty vector control or pCMX3b-flag-V expression plasmid, harvested 48 h

853 p.t. and subjected to a guanidinium chloride buffer. 6His-SUMO conjugates were
854 purified using a Ni-NTA-matrix (Ni-NTA pull down) and input represents total-cell
855 lysates. Samples were separated by SDS-PAGE and visualized by immunoblotting.
856 Ni-NTA purified and input proteins were detected using mab M2 (α-flag), mab α-
857 6His and mab AC-15 (α-β-actin). Molecular weights in kDa are indicated on the left,
858 while corresponding proteins are labeled on the right, (exp. = exposure). (**B**) HeLa
859 cells or HeLa cells stably expressing 6His-SUMO2 were transfected with 10 µg of
860 empty vector control or pCMX3b-flag-V expression plasmid and superinfected with
861 H5*pg*4100 (moi 20) 24 h p.t. .The cells were harvested 24 h p.i. and subjected to a
862 guanidinium chloride buffer. 6His-SUMO conjugates purified by Ni-NTA pull down,
863 and input total-cell lysates, were resolved by SDS-PAGE and visualized by
864 immunoblotting. Ni-NTA purified and input proteins were detected using pab α-V,
865 mab α-6His and mab AC-15 (α-β-actin). Molecular weights in kDa are indicated on
866 the left, while corresponding proteins are labeled on the right.
867
868 **Figure 3. Identification of protein V SUMOylation sites.** (**A**) *In silico* analysis of
869 **protein V** to determine potential SUMO conjugation or interaction motifs, using the
870 algorithms *SUMOPlot*™ (http://www.abgent.com/sumoplot), *GPS-SUMO* and
871 *Jassa*. (**B**) Schematic illustration of the **protein V** SCM mutants used in the
872 experiments. SCM are depicted in pink, nSCM in green and K→R exchanges in
873 yellow. (**C**) HeLa cells or HeLa cells stably expressing 6His-SUMO2, were transfected
874 with either 10 µg empty vector control, pCMX3b-flag-V expression plasmid or flag-V
875 SCM mutants as indicated. Cells were harvested 48 h p.t. and subjected to a
876 guanidinium chloride buffer. 6His-SUMO conjugates purified by using Ni-NTA pull

down, and input of total-cell lysates were resolved by SDS-PAGE and visualized by immunoblotting. Ni-NTA-purified and input proteins were detected using mab M2 (α-flag), mab α-6His and mab AC-15 (α-β-actin). Molecular weights in kDa are indicated on the left, while corresponding proteins are labeled on the right.

Figure 4. Protein V SUMOylation modulates intracellular distribution of the viral factor. (**A, B**) 6His-SUMO2 HeLa cells were transfected with 2 µg of a pCMX3b-flag-V expression plasmid, the different flag-V SCM mutants or the empty vector control and fixed with MeOH 48 h p.t. The cells were stained with pab α-V, which was detected with an Alexa488-conjugated (green) secondary antibody, while nuclei were stained with dapi (blue). *Merge* indicates the overlay of single images in each row. Images were captured with a Leica fluorescence wide field microscope. Statistical summary of the captured phenotypes (n), is shown below in comparison to Hela and HepaRG cells (A) or on the right (B).

Figure 5. Generation of a replication-competent protein V SUMO mutant viruses. (A) A bacmid containing the whole genome of HAdV (pH5*pg*4100), was divided into seven parts by restriction enzymes cutting only one unique site of the viral genome. The resulting fragments of the viral genome were subcloned into vector plasmids that allow the introduction of point mutations or other alterations by site-directed mutagenesis using QC PCRs. The modified fragment of viral DNA can be cloned back into the viral genome. The newly derived bacmid DNA can be multiplied in bacteria and linearized with the restriction enzyme *Pac*I, which deletes the non-viral part. The linearized, ds viral genome is transfected into human cells to produce

infectious particles of the desired virus mutant. (**B**) HAdV-C5 **protein V** is part of genome fragment L3, where we introduced single nt-exchanges in the **protein V** coding sequence leading to K→R exchanges within the three SCM and one neighboring nSCM of the protein. (**C**) HeLa cells stably expressing 6His-SUMO2 were infected with HAdV wt (H5*pg*4100, moi 5) or the HAdV **protein V** SCM mutant (H5*pm*4242, moi 5). The cells were harvested 24 h p.i. and subjected to a guanidinium chloride buffer. 6His-SUMO conjugates purified by Ni-NTA pull down, plus control input of total-cell lysate were resolved by SDS-PAGE and visualized by immunoblotting. Ni-NTA purified and input proteins were detected using pab α-V, mab α-6His, mab B6-8 (α-E2A) and mab AC-15 (α-β-actin). Molecular weights in kDa are indicated on the left, while corresponding proteins are labeled on the right. Mock means uninfected control.

Figure 6. Role of protein V SUMOylation during productive infection. (**A**) HepaRG cells (H1299cells; see (C)) were infected with HAdV wt (H5*pg*4100, moi 20) or protein V SCM mutant virus (H5*pm*4242, moi 20) and harvested 24, 48 or 72 h p.i. Viral progeny were isolated and titrated by visualizing the infected cells via immunofluorescence to determine the yield. The average of n = 3 independent experiments, each done in triplicate, were plotted on bar graphs to emphasize the ratio of the protein V SCM mutant virus and HAdV wt (H5*pm*4242/H5*pg*4100) at each time point investigated. Error bars indicate the standard deviation; ffu = fluorescence forming units. (**B**) HepaRG cells (H1299cells; see (D)) were infected with HAdV wt (H5*pg*4100, moi 20) or protein V SCM mutant virus (H5*pm*4242, moi 20) and harvested 8, 16, 24, 48 or 72 h p.i. Total-cell lysates were resolved by SDS-PAGE

925 and visualized by immunoblotting. Proteins were detected using mab M73 (α-E1A),
926 pab α-19K, mab 2A6 (α-E1B-55K), mab B6-8 (α-E2A), mab RSA3 (α-E4orf6), mab 6B10
927 (α-L4-100K), pab α-V, pab L133 (α-capsid), mab DO-1 (α-p53) and mab AC-15 (α-β-
928 actin). Molecular weights in kDa are indicated on the left, while corresponding
929 proteins are labeled on the right. Mock means uninfected control. (**C**) HepaRG cells
930 were infected with HAdV wt (H5*pg*4100, moi 20) or **protein V** SCM mutant virus
931 (H5*pm*4242, moi 20) and harvested 6, 12 or 24 h p.i. Total RNA was isolated from the
932 cells, mRNA was reversely transcribed and the resulting cDNA was amplified by RT-
933 PCR with primer pairs specific for a certain viral sequence and primer pairs against a
934 cds-fragment of cellular 18S rRNA (Tab. 1). HAdV mRNA amounts are depicted
935 relative to the amounts of cellular 18S rRNA as an average of n = 3 independent
936 experiments. Error bars indicate the standard deviation. RT-PCR was performed in
937 technical duplicates for each experiment and the statistics were calculated with a 2-
938 tailed, unpaired t-test for each time point. P-value < 0.05 = *.On the right, the ratio of
939 the **protein V** SCM mutant virus and HAdV wt (H5*pm*4242/H5*pg*4100) is illustrated
940 for each time point investigated.
941
942 **Figure 7. SUMO conjugation promotes protein V nucleoli association.** HepaRG
943 cells were infected with HAdV wt (H5*pg*4100, moi 20) or HAdV protein V SCM
944 mutant (H5*pm*4242, moi 20) and fixed with 4% PFA 24 h p.i. To visualize protein V
945 the cells were treated with pab α-V. **(A)** E1A was visualized with mab M73 (α-E1A),
946 (**B)** E1B-55K was visualized with mab 2A6 (α-E1B-55K) and (**C)** E2A was visualized
947 with mab B6-8 (α-E2A). Primary antibodies were detected with Alexa488- (green) or
948 Cy3- (red) conjugated secondary antibodies and nuclei were stained with dapi (blue).

949 *Merge* indicates the overlay of single images of each row and mock means uninfected
950 control. Images were captured with a Nikon confocal microscope. The colocalization
951 of HAdV protein V and E2A is depicted by 2D-histograms, which correlate the pixel
952 intensities of two channels, on the left and the corresponding channel overlay of the
953 analyzed regions of interest on the right, tM means thresholded *Mander's split*
954 *coefficient* where number 1 corresponds to the red channel (protein V) and number 2
955 corresponds to the green channel (E2A). (**D)** The experimental conditions for
956 individual experiments 1-4; examples from experimental condition 1 are shown in A-
957 C. (**E**) Statistical summary of captured phenotypes in n = 4 independent
958 experiments.
959
960 **Figure 8. Reducing protein V SUMOylation promotes viral DNA synthesis.** (**A**)
961 HepaRG cells were infected with HAdV wt (H5*pg*4100, moi 20) or protein V SCM
962 mutant virus (H5*pm*4242, moi 20) and harvested 1, 16, 24 or 48 h p.i.. Genomic DNA
963 was isolated from the cells and amplified by RT-PCR with primer pairs specific for a
964 HAdV-C5 hexon-cds fragment or specific for a fragment of the cellular single copy
965 gene β2-microglobuline (Tab. 1). HAdV DNA amounts are depicted relative to the
966 amounts of the cellular single copy gene as an average from n = 4 independent
967 experiments. Error bars indicate the standard deviation. RT-PCR was performed in
968 technical duplicates for each experiment and statistics were calculated with a 2-
969 tailed, unpaired t-test. P-value < 0.05 means *. (**B)** The ratio of the protein V SCM
970 mutant virus and HAdV wt (H5*pm*4242/H5*pg*4100) at each time point investigated.

Figure 1
Freudenberger et al.

A

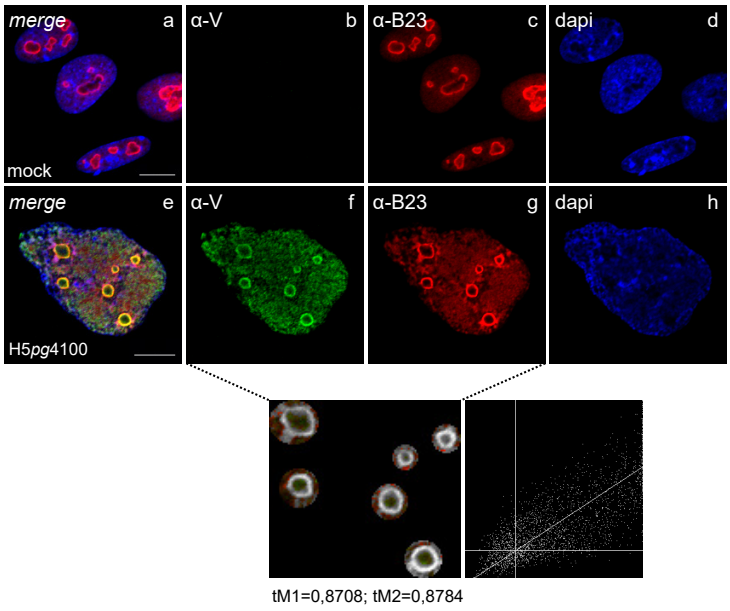

B

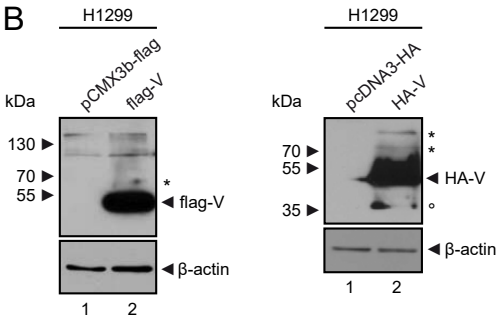

Journal of Virology

JVI

Journal of Virology

Figure 2
Freudenberger et al.

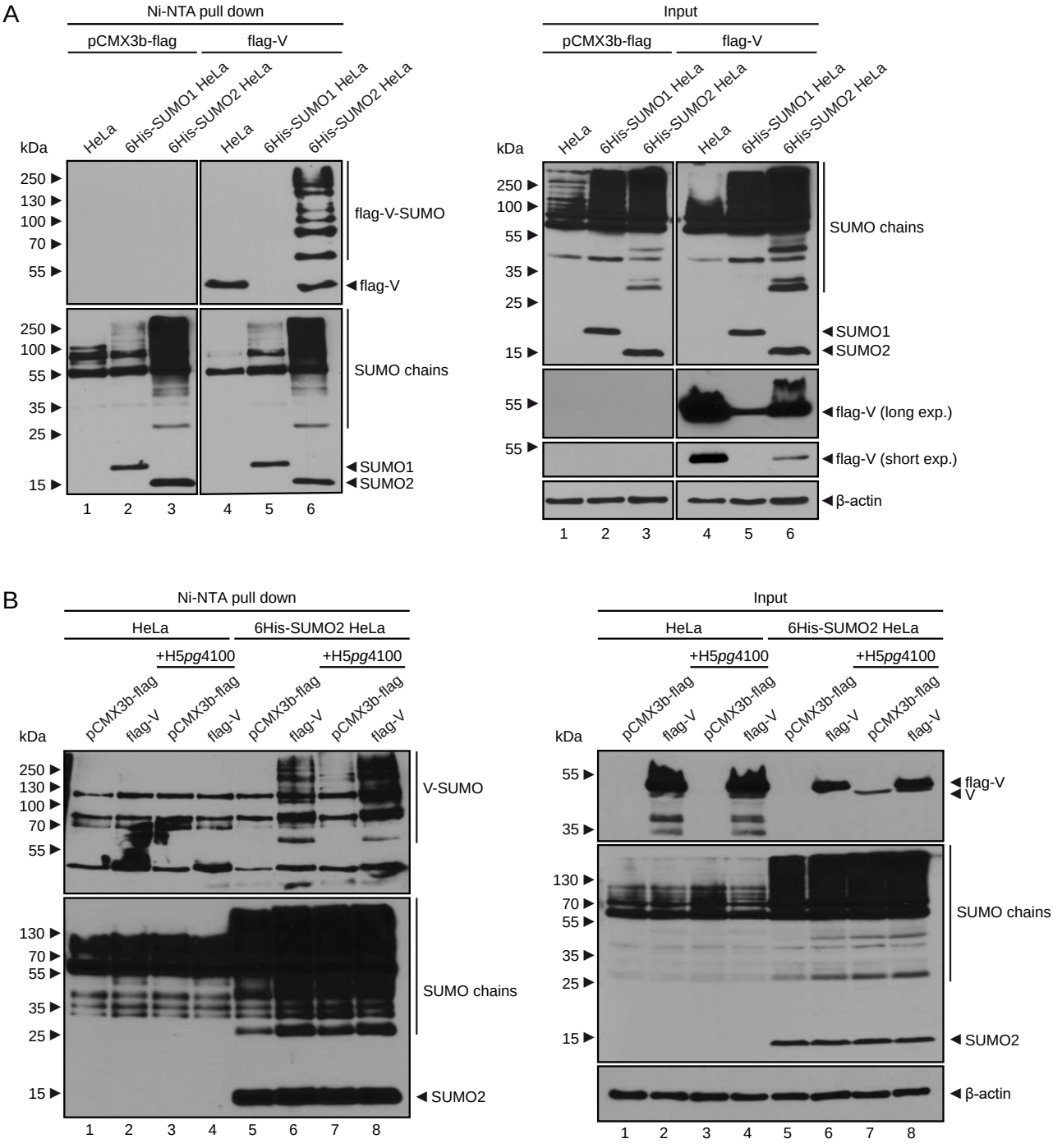

Journal of Virology

JVI

Journal of Virology

Figure 3
Freudenberger et al.

A

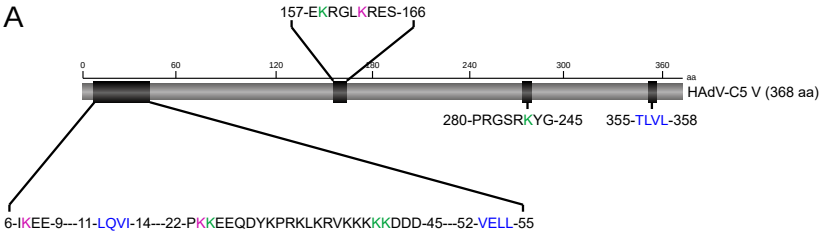

consensus SUMO conjugation motif (SCM): ψ-K-x-E/D
SUMO interacting motif (SIM)
non-consensus SUMO conjugation motif (nSCM)

B

SUMO-motif	K→R-exchange	designation
6-IKEE-9	6-IREE-9	HAdV-C5 VK7R
22-PKKEE-26	22-PRREE-26	HAdV-C5 VK23/24/R
161-LKRE-164	161-LRRE-164	HAdV-C5 VK162R
K7+K23/24	R7+R23/24	HAdV-C5 VK7/23/24R
K23/24+K162	R23/24+R162	HAdV-C5 VK23/24/162R
K7+K162	R7+R162	HAdV-C5 VK7/162R
K7+K23/24+K162	R7+R23/24+R162	HAdV-C5 V4xKR

C

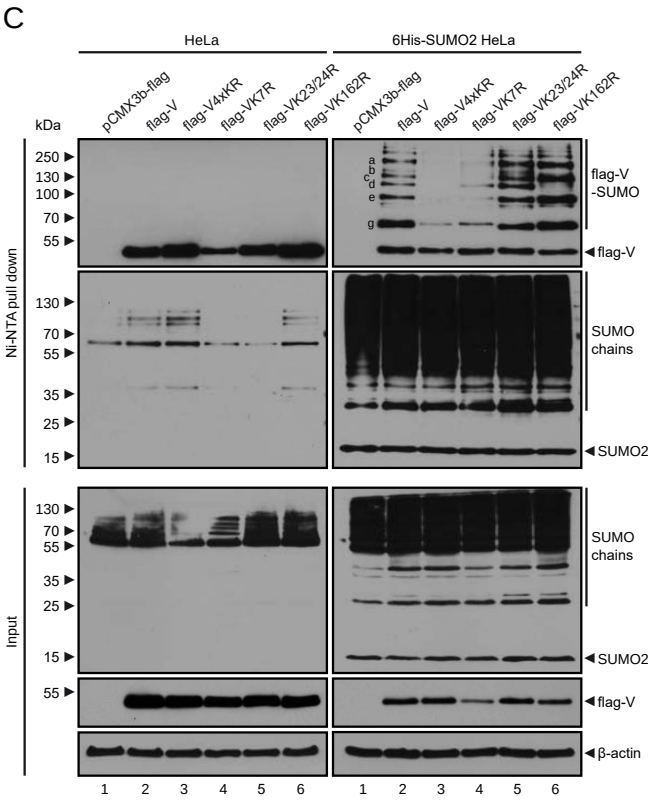

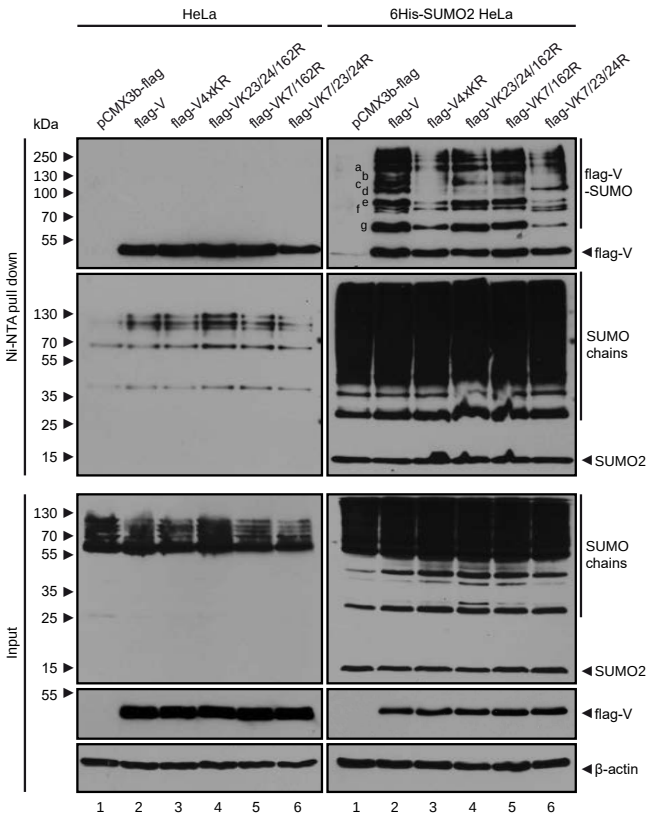

Figure 4
Freudenberger et al.

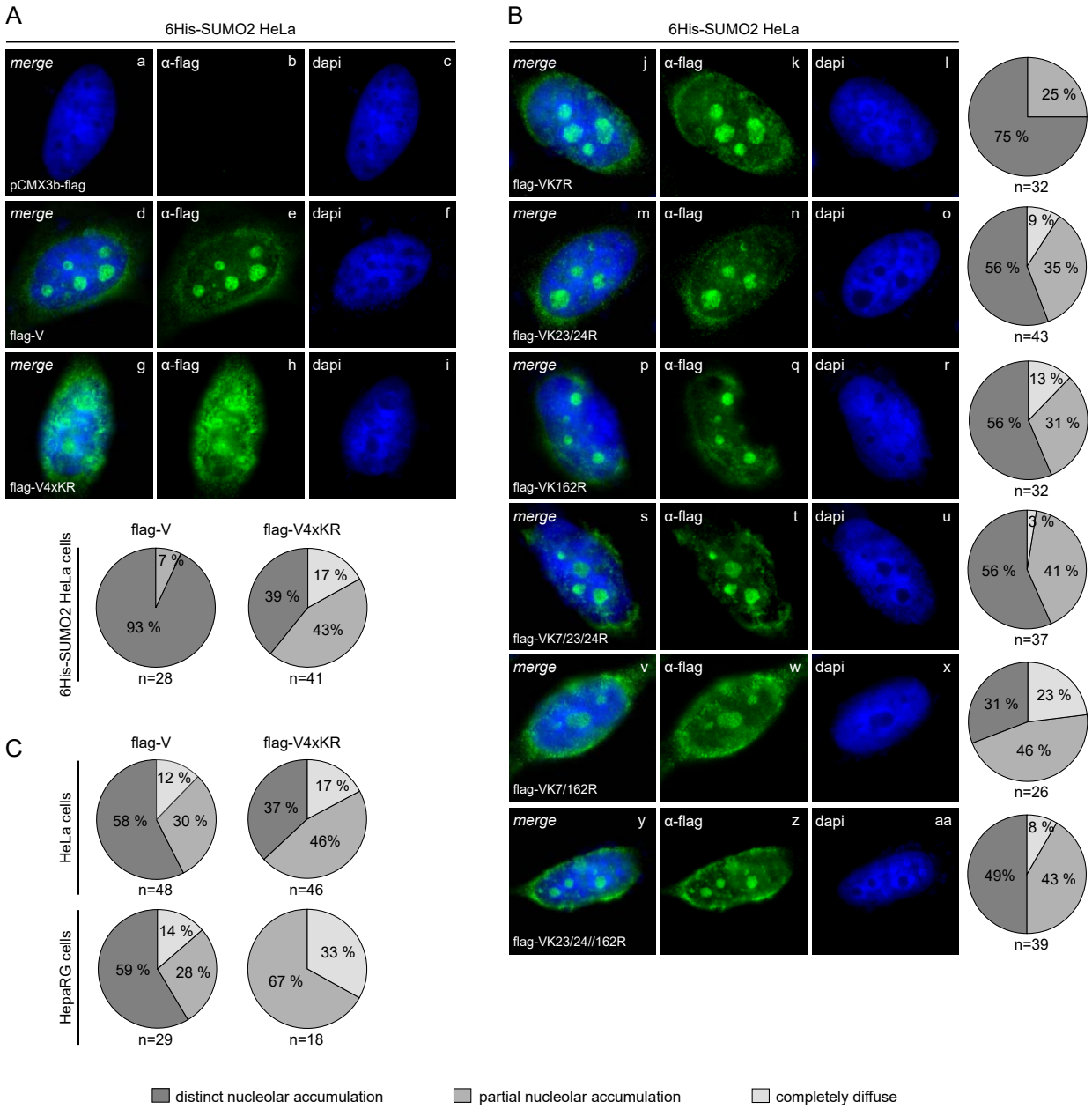

Figure 5
Freudenberger et al.

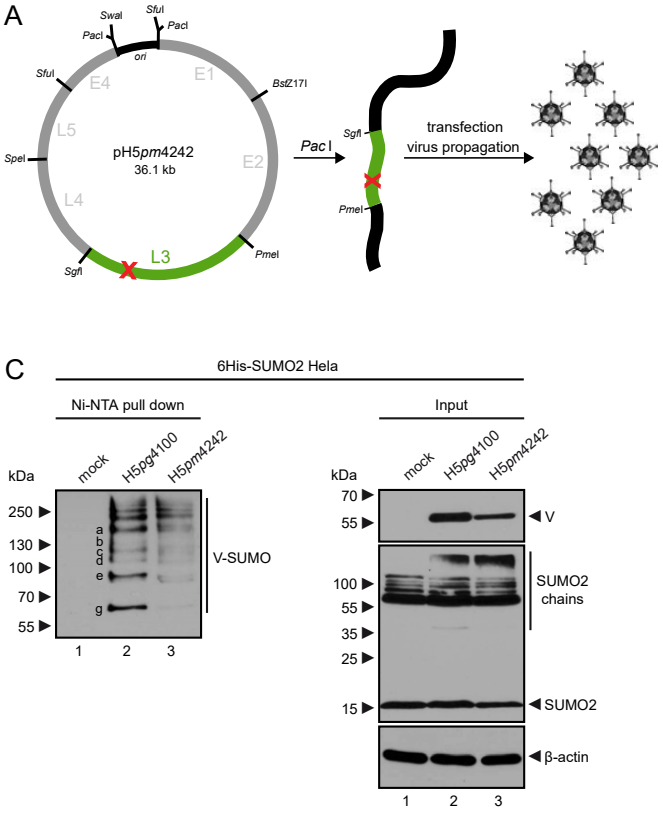

Figure 6
Freudenberger et al.

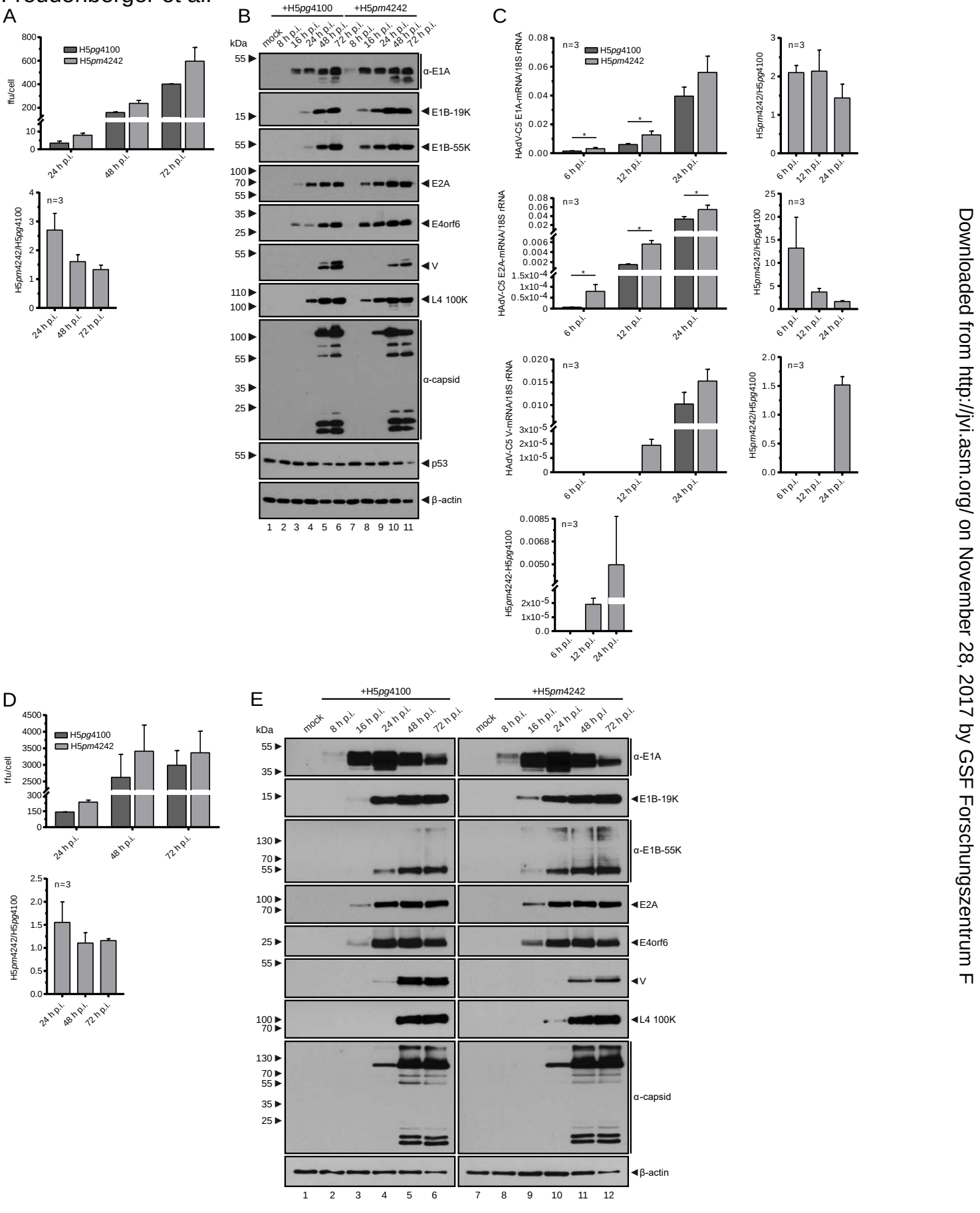

Figure 7
Freudenberger et al.

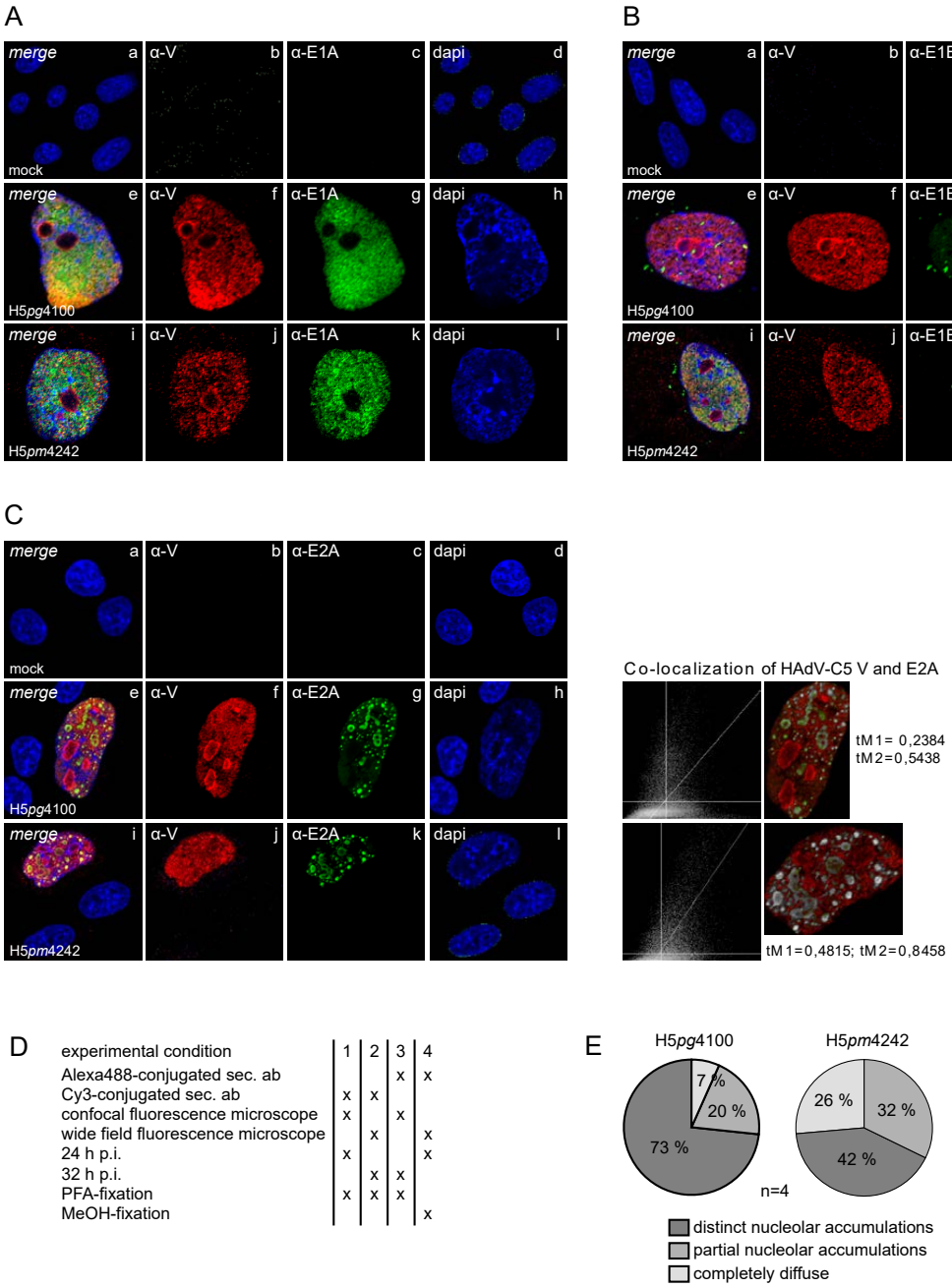

D

experimental condition	1	2	3	4
Alexa488-conjugated sec. ab			x	x
Cy3-conjugated sec. ab	x	x		
confocal fluorescence microscope	x		x	
wide field fluorescence microscope		x		x
24 h p.i.	x			x
32 h p.i.		x	x	
PFA-fixation	x	x	x	
MeOH-fixation				x

Figure 8
Freudenberger et al.